ACS Energy LETTERS

http://pubs.acs.org/journal/aelccp

LETTER

Rutile TiO_2 as an Anode Material for Water-Splitting Dye-Sensitized Photoelectrochemical Cells

John R. Swierk,* Kevin P. Regan, Jianbing Jiang, Gary W. Brudvig, and Charles A. Schmuttenmaer*

Department of Chemistry and Yale Energy Sciences Institute, Yale University, New Haven, Connecticut 06520-8107, United States

Supporting Information

ABSTRACT: **Water-splitting dye-sensitized photoelectrochemical cells (WS-DSPECs) use a wide bandgap metal oxide semiconductor functionalized with a light-absorbing dye and water-oxidation catalyst to harvest light and drive water oxidation, respectively. We demonstrate here that the rutile polymorph of TiO_2 (r-TiO_2) is a promising anode material for WS-DSPECs. Recombination between the injected electron and oxidized sensitizer with r-TiO_2 is an order of magnitude slower than with anatase TiO_2 (a-TiO_2), with injection yields approaching 100%. Studies with a reductive quencher demonstrate that r-TiO_2 is significantly more efficient than a-TiO_2, while exhibiting greater dye stability. Furthermore, comparison of direct band gap excitation photocurrent generation for bare and sensitized r-TiO_2 suggests that the sensitizer functions as a light harvester and redox mediator.**

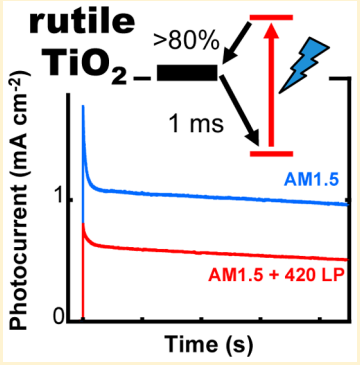

Efficient conversion of solar energy into a readily stored fuel is a significant scientific challenge. Water-splitting dye-sensitized photoelectrochemical cells (WS-DSPECs) accomplish this task using a mesoporous, nanoparticulate metal oxide film functionalized with a light-absorbing sensitizer and a water-oxidation catalyst.[1,2] Under illumination, the sensitizer absorbs light and then transfers an excited electron to the conduction band (CB) of the oxide. The oxidized sensitizer either transfers a hole to the catalyst or triggers a series of intermolecular, cross-surface hole transfers to oxidize a catalyst.[3,4] At the same time, the injected electrons diffuse through the metal oxide until reaching a transparent conducting back contact which is electrically connected to a dark cathode.[5]

WS-DSPEC efficiencies with the most common oxide support, anatase TiO_2 (a-TiO_2), are limited by low injection yields (20−30%) and rapid back-electron recombination from the CB.[6] In SnO_2, the CB is roughly 0.5 V more positive (i.e., lower in energy) than the CB of a-TiO_2, which leads to injection yields of ∼100%.[7] Unfortunately, recombination of the injected electron and oxidized sensitizer is known to be significantly faster in SnO_2.[8,9] While SnO_2-core/TiO_2-shell electrodes[10,11] show promise as a strategy to retard recombination from SnO_2, the TiO_2-shell slows the injection kinetics and reduces the injection yield.[7]

The rutile polymorph of TiO_2 (r-TiO_2) is an attractive, though unexplored, oxide material for use in WS-DSPECs. In particular, the CB edge in r-TiO_2 is approximately 0.2 V below the a-TiO_2 CB,[12] providing an increased driving force for injection. In addition, the CB in r-TiO_2 is primarily composed of d-orbitals[13] and should promote rapid injection kinetics because there is a high density of states.[14] Furthermore, charge carrier lifetimes in r-TiO_2 are known to be significantly longer than in a-TiO_2.[15] Though the electron diffusion coefficient of r-TiO_2 is about an order of magnitude lower than that of a-TiO_2, dye-sensitized solar cells prepared from r-TiO_2 exhibit photovoltaic performance comparable to that of cells prepared from anatase.[16] While the CB of r-TiO_2 is too positive to drive proton reduction and thus requires an external bias or use of a photocathode, this is the case in all extant WS-DSPECs. Because of fast recombination and poor injection in a-TiO_2, its Fermi level typically sits positive of the H^+/H_2 under illumination and requires a bias voltage to produce any meaningful photocurrent.[6]

In this Letter, we use a common WS-DSPEC sensitizer ((4,4′-diphosphonato-2,2′-bipyridine)bis(2,2′-bipyridine)-ruthenium(II) bromide, **RuP**) to demonstrate that sensitized r-TiO_2 exhibits injection yields approaching 100%, while the recombination kinetics are an order of magnitude slower than that of sensitized anatase. Furthermore, the efficient injection and slow recombination manifests in significantly better photoelectrochemical performance for r-TiO_2 in studies with a reductive scavenger (hydroquinone, H_2Q). The use of H_2Q allows us to eliminate dye catalyst interactions that can

Received: July 14, 2016
Accepted: August 23, 2016
Published: August 23, 2016

DOI: 10.1021/acsenergylett.6b00279
ACS Energy Lett. 2016, 1, 603−606

complicate analyses of device performance and demonstrates the advantages of r-TiO_2 over a-TiO_2.[10,17]

Rutile particles were synthesized using the method of Park et al.[16] and prepared as a paste for doctor-blading (see the Supporting Information). Powder X-ray diffraction shows that the sintered particles are phase pure r-TiO_2 (Figure S1), with no evidence of a-TiO_2. An average crystallite size of 13 ± 0.6 nm was calculated from the X-ray diffraction pattern using the Scherrer equation (Figure S2). Transmission electron microscopy shows the particles are single crystals and have a rodlike structure with an average length of 63 ± 3 nm and an average width of 18 ± 1 nm (Figure S3).

Bare films show a scattering baseline at long wavelengths (>600 nm) and strong attenuation at wavelengths less than 500 nm (Figure S4). That feature is likely to be a combination of scattering and direct bandgap excitation as the bandgap of r-TiO_2 corresponds to 413 nm. RuP-sensitized films were prepared by soaking the bare r-TiO_2 films in a 0.1 mM solution of RuP in anhydrous ethanol for 22 h. After sensitization, a new absorption peak can be observed centered at 460 nm (Figure S4). By subtracting the bare rutile spectrum from the RuP-sensitized spectrum, we determine a dye loading of 6.1 ± 0.5 × 10^{-9} mol cm^{-2} μm^{-1}. Under identical sensitizing conditions, we determined a loading of 9.4 ± 0.8 × 10^{-9} mol cm^{-2} μm^{-1} on a-TiO_2.[5] The a-TiO_2 particle size in those films was approximately 20 nm,[18] suggesting the difference in dye loading between a-TiO_2 and r-TiO_2 is due to decreased surface area in r-TiO_2. We also assessed the stability of RuP-sensitized r-TiO_2 at pH 6 using the method of Hanson et al.[19] wherein the absorbance of the sample is monitored as a function of time under continuous illumination at 470 nm. The rate constant for desorption (k_{des}) was measured to be 2.1 (± 0.7) × 10^{-5} s^{-1} (Figure S5). This value is comparable with that of RuP-sensitized a-TiO_2 at pH 1 (5 × 10^{-5} s^{-1}). Near neutral pH, RuP rapidly desorbs from a-TiO_2 unless an overcoat of Al_2O_3 is applied.[20]

One of the most significant limits on WS-DSPECs is fast recombination of injected electrons with the oxidized sensitizer. We recently estimated that less than 2% of injected electrons persist to sufficiently long time scale (>100 μs) to contribute to water-oxidation activity.[6,21] To characterize recombination, we utilized transient-absorption spectroscopy (TAS). Following a ∼7 ns laser pulse, injection of photoexcited electrons into the r-TiO_2 CB results in a bleach of the strong RuP metal-to-ligand charge-transfer (MLCT) band centered at ∼460 nm (Figure 1, blue trace).[8] Recombination can be observed by monitoring the recovery of the MLCT band on the nano- to millisecond time scale. For this study, a 532 nm pulse (3.82 mJ cm^{-2}) was used to photoexcite the RuP sensitizer. Figure 1 shows a representative single-wavelength TAS scan monitored at 460 nm for RuP-sensitized r-TiO_2. The laser pulse occurs at t = 0, resulting in a large initial bleach upon photoinjection. The injection kinetics cannot be resolved given the ∼7 ns instrument response function of our TA spectrometer. We also examined bare r-TiO_2 (Figure 1, black trace), which exhibited little transient response when probed at 460 nm. As a point of comparison, we also measured RuP-sensitized a-TiO_2 (Figure 1, red trace) with 4 Å Al_2O_3 deposited over the sensitized a-TiO_2 to stabilize the dye at pH 6. We utilized a 4 μm film of a-TiO_2 to match the dye loading with r-TiO_2 and manually adjusted the laser power to match the total number of injected electrons between a-TiO_2 and r-TiO_2. We observed

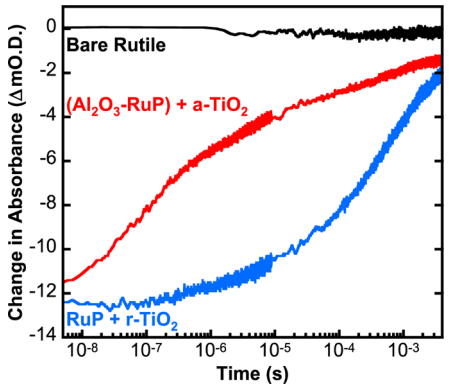

Figure 1. Representative single-wavelength transient-absorbance trace of a RuP-sensitized 7 μm r-TiO_2 film (blue trace), RuP-sensitized 4 μm a-TiO_2 film coated with 4 Å Al_2O_3 (red trace), and bare 7 μm r-TiO_2 film in 0.1 M KNO_3 excited at 532 nm (3.82 mJ cm^{-2} pulse energy, 10 Hz) and monitored at 460 nm using a 460 ± 10 nm bandpass filter.

negligible loss of dye from the r-TiO_2 or the Al_2O_3-coated a-TiO_2 over the course of the TAS experiment.

The single-wavelength traces were fit to a stretched-exponential equation:

$$\Delta A = \Delta A_0 \exp\left[-\left(\frac{t}{\tau}\right)^{\beta}\right] + \Delta A_C \quad (1)$$

where ΔA_0 is the change in absorbance at t = 0, τ the lifetime, β a stretching parameter ($0 < \beta < 1$), and ΔA_C a long-time offset. The β parameter is inversely related to the distribution of rates, and when β = 1, the stretched-exponential equation becomes a single-exponential equation.[22] We can determine a recombination rate constant, k_{rec}, by taking the reciprocal of $\langle\tau\rangle$, which is defined as

$$\langle\tau\rangle = \frac{\tau}{\beta}\Gamma\left(\frac{1}{\beta}\right) \quad (2)$$

where Γ is the gamma function. From the fits of the single-wavelength traces, we determine a k_{rec} of 2.5 ± 1.1 × 10^3 s^{-1} for r-TiO_2 and 2.9 ± 0.6 × 10^4 s^{-1} for a-TiO_2.

The slower recombination lifetime on r-TiO_2 has direct implications for device performance. Except for the sensitizer molecules immediately adjacent to a catalytic site, holes generated by electron injection must undergo a series of intermolecular electron-transfer events to reach the catalyst. The average distance a hole can travel to reach a catalyst site is given by the recombination time and the cross-surface hole diffusion coefficient.[6] Slowing the recombination by an order of magnitude results in a ∼5-fold increase in the area around a catalytic site where a hole can be generated and have a reasonable chance of encountering a catalytic site. Only holes that reach a catalyst contribute to photocurrent generation; therefore, an increase in recombination time should result in an increase in induced photocurrent.

Beyond fast recombination, low injection yields fundamentally limit the performance of WS-DSPECs using a-TiO_2. Previously, we determined an injection yield of 0.2−0.3 for RuP on a-TiO_2 at pH 6.8,[7,23] meaning that at best 20−30% of absorbed photons are converted into photocurrent. We estimated the injection yield for RuP on r-TiO_2 from the bleach at t = 0 (see the Supporting Information) and calculated

DOI: 10.1021/acsenergylett.6b00279
ACS Energy Lett. 2016, 1, 603−606

an average injection yield of 0.74 ± 0.13. This likely represents a lower limit on the injection yield because we do not account for reflection or scattering losses of excitation intensity. A detailed study on the injection kinetics and yields for r-TiO_2 is planned.

Photocurrent generation in a WS-DSPEC is the net result of a series of electron-transfer and transport events (injection, recombination, dye regeneration, etc.). Poor performance at any given step can limit the observed photocurrent. Specifically, slow regeneration of the oxidized dye by the catalyst or scavenging of CB electrons by the catalyst can play a significant role in reducing performance and are highly dependent on the specific catalyst.[18] To assess the potential utility of r-TiO_2 as a photoanode material in WS-DSPECs, we utilize $\mathbf{H_2Q}$ to eliminate secondary interactions related to the catalyst and study the performance of sensitized rutile in the limit of rapid sensitizer regeneration.[10] For a representative sample under one-sun illumination (using an AM1.5 filter), we observe a peak photocurrent of 1.5 mA cm^{-2}, which decays to roughly 1 mA cm^{-2} over the course of 15 min (Figure 2, blue line). To

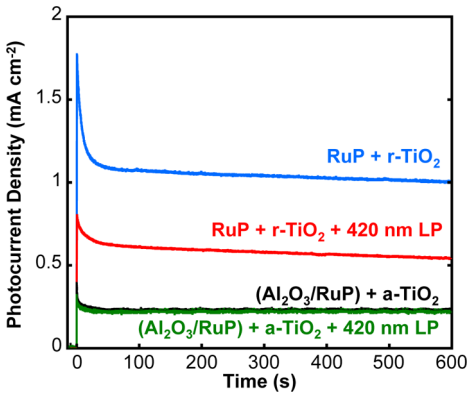

Figure 2. Chronoamperometry of a RuP-sensitized r-TiO_2 film (red and blue traces) and RuP-sensitized a-TiO_2 (black and green traces) at 0.1 V vs. Ag/AgCl (sat. NaCl) in a 0.1 M pH 6.8 potassium phosphate buffer with 0.5 M KNO_3 and 20 mM hydroquinone added. Illumination from a 300 W Xe lamp fitted with an AM1.5 filter (blue and black traces) and an AM1.5 filter plus a 420 nm long-pass filter (red and green traces).

eliminate the contribution of direct bandgap excitation, we also measured the current under the same illumination conditions with a 420 nm long-pass filter. Addition of the long-pass filter resulted in a 50% reduction in the generated photocurrent. This suggests that approximately 500 μA cm^{-2} of photocurrent is generated through direct band gap excitation. At full AM1.5 illumination, similarly RuP-sensitized, Al_2O_3-coated a-TiO_2 electrodes exhibit an initial spike of ∼300 μA cm^{-2} of photocurrent, which decays to a stable output of ∼230 μA cm^{-2} (Figure 2, black trace). Interestingly, when a 420 nm long-pass is added, we see only a slight drop in the stable current to ∼220 μA cm^{-2} (Figure 2, green trace). These results suggest that even with a fast reductive scavenger the poor injection yields and fast recombination of sensitized a-TiO_2 prevent efficient photocurrent generation under these conditions.

Lapides et al.[17] studied RuP-sensitized a-TiO_2 with $\mathbf{H_2Q}$ and observed an initial photocurrent of ∼1.5 mA cm^{-2} followed by a rapid polarization to less than 0.6 mA cm^{-2} in 30 s. Importantly, their study was conducted at pH 4.7 where injection from RuP should be considerably more favorable. As in this study, a thin overcoat of Al_2O_3 was necessary for stable photocurrent generation because in the presence of oxygen RuP rapidly desorbs from a-TiO_2 at near neutral pH.[19] In contrast, during both the transient absorption and photoelectrochemical studies (which are conducted in ambient air), we observe a minimal loss of dye from RuP-sensitized r-TiO_2 after sustained illumination (Figure S4, green line). This highlights one of the major advantages that r-TiO_2 offers over a-TiO_2, namely that in the pH range that is necessary to drive water-splitting, RuP-sensitized r-TiO_2 is stable without having to add any additional overlayers.

While $\mathbf{H_2Q}$ scavenging is not diffusion limited under these conditions, it serves to mimic the behavior of a water-oxidation catalyst that can efficiently regenerate the oxidized sensitizer. That sensitized a-TiO_2 generates significantly less photocurrent than sensitized r-TiO_2 demonstrates how the improved injection and recombination kinetics of r-TiO_2 combine to enhance device performance. We note that the $\mathbf{H_2Q}$ currents observed with r-TiO_2 should not be taken as the maximum achievable currents. RuP absorbs strongly only at wavelengths <500 nm, and we have not maximized light harvesting in that spectral window (Figure S4).

Surprisingly, when we use $\mathbf{H_2Q}$ with a bare r-TiO_2 electrode under full AM1.5 one-sun illumination, we observe only about 75 μA cm^{-2}, and less than 1 μA cm^{-2} when the 420 nm long-pass filter is added (Figure S6). The latter result confirms that, with a 420 nm long-pass filter, the photocurrent we observe with RuP-sensitized r-TiO_2 is almost entirely due to the sensitizer. However, the significant difference in photocurrent attributed to direct band gap excitation of the sensitized r-TiO_2 (500 μA cm^{-2}) and the photocurrent generated by the bare r-TiO_2 under full illumination suggests that the chromophore plays an additional role beyond photosensitizer. Only a small fraction of the 500 μA cm^{-2} difference is likely related to injection from photoexcited RuP, because RuP exhibits a local absorption minimum around 400 nm,[3] while the bandgap of r-TiO_2 corresponds to an absorption of about 413 nm, making absorption by r-TiO_2 more likely. Furthermore, as we demonstrated with RuP on the wider bandgap a-TiO_2, the dye contributes little photocurrent at wavelengths shorter than 420 nm. On the basis of this, we suggest that the current enhancement in the presence of RuP may arise at least in part because the RuP can act as a redox mediator for holes in the valence band of r-TiO_2. At pH 6.8, the valence band of r-TiO_2 lies close to 2.6 V vs NHE. Under direct bandgap excitation, the hole created in the valence band can readily oxidize RuP ($E_{1/2}^{RuIII/RuII}$ = 1.33 V vs NHE), moving the hole onto the surface, thereby creating a charge-separated state. Further work is needed to fully understand this potential mechanism.

Addressing both low injection and fast recombination rates are paramount to the development of efficient WS-DSPECs, and r-TiO_2 represents a significant step in this direction. Sensitized r-TiO_2 exhibits recombination kinetics that are an order of magnitude slower than that of a-TiO_2, while at the same time the injection yield for RuP into r-TiO_2 approaches unity at near neutral pH conditions. Photoelectrochemical studies with a reductive scavenger, $\mathbf{H_2Q}$, demonstrate that in the limit of rapid dye regeneration r-TiO_2 significantly outperforms anatase, while exhibiting enhanced dye stability. The results with $\mathbf{H_2Q}$ also suggest that RuP may also act as a redox mediator for holes generated by direct bandgap

DOI: 10.1021/acsenergylett.6b00279
ACS Energy Lett. 2016, 1, 603−606

excitation. Taken together, these results demonstrate that r-TiO_2 is a very promising photoanode material for WS-DSPECs.

■ ASSOCIATED CONTENT

Supporting Information

The Supporting Information is available free of charge on the ACS Publications website at DOI: 10.1021/acsenergylett.6b00279.

Detailed experimental procedures, powder XRD data of sintered r-TiO_2, TEM micrograph of rutile particles, UV−visible spectra of bare and sensitized r-TiO_2, difference spectrum of bare and sensitized r-TiO_2, and photoelectrotrolyis of bare r-TiO_2 in H_2Q (PDF)

■ AUTHOR INFORMATION

Corresponding Authors

*E-mail: jrswierk@gmail.com.

*E-mail: charles.schmuttenmaer@yale.edu.

Notes

The authors declare no competing financial interest.

■ ACKNOWLEDGMENTS

The authors thank Nicholas McCool for helpful discussion during the preparation of this Letter as well as assistance with the atomic layer deposition of Al_2O_3. This work was funded by the U.S. Department of Energy Office of Science, Office of Basic Energy Sciences, under award DE-FG02-07ER15909 and by a generous donation from the TomKat Charitable Trust.

■ REFERENCES

(1) Swierk, J. R.; Mallouk, T. E. Design and Development of Photoanodes for Water-Splitting Dye-Sensitized Photoelectrochemical Cells. *Chem. Soc. Rev.* **2013**, *42*, 2357−2387.

(2) Youngblood, W. J.; Lee, S.-H. A.; Kobayashi, Y.; Hernandez-Pagan, E. A.; Hoertz, P. G.; Moore, T. A.; Moore, A. L.; Gust, D.; Mallouk, T. E. Photoassisted Overall Water Splitting in a Visible Light-Absorbing Dye-Sensitized Photoelectrochemical Cell. *J. Am. Chem. Soc.* **2009**, *131*, 926−927.

(3) Hanson, K.; Brennaman, M. K.; Ito, A.; Luo, H.; Song, W.; Parker, K. A.; Ghosh, R.; Norris, M. R.; Glasson, C. R. K.; Concepcion, J. J.; et al. Structure-Property Relationships in Phosphonate-Derivatized, Ru^{II} Polypyridyl Dyes on Metal Oxide Surfaces in an Aqueous Environment. *J. Phys. Chem. C* **2012**, *116*, 14837−14847.

(4) Brennan, B. J.; Durrell, A. C.; Koepf, M.; Crabtree, R. H.; Brudvig, G. W. Towards Multielectron Photocatalysis: a Porphyrin Array for Lateral Hole Transfer and Capture on a Metal Oxide Surface. *Phys. Chem. Chem. Phys.* **2015**, *17*, 12728−12734.

(5) Swierk, J. R.; McCool, N. S.; Saunders, T. P.; Barber, G. D.; Mallouk, T. E. Effects of Electron Trapping and Protonation on the Efficiency of Water-Splitting Dye-Sensitized Solar Cells. *J. Am. Chem. Soc.* **2014**, *136*, 10974−10982.

(6) Swierk, J. R.; McCool, N. S.; Mallouk, T. E. Dynamics of Electron Recombination and Transport in Water-Splitting Dye-Sensitized Photoanodes. *J. Phys. Chem. C* **2015**, *119*, 13858−13867.

(7) Swierk, J. R.; McCool, N. S.; Nemes, C. T.; Mallouk, T. E.; Schmuttenmaer, C. A. Ultrafast Electron Injection Dynamics of Photoanodes for Water-Splitting Dye-Sensitized Photoelectrochemical Cells. *J. Phys. Chem. C* **2016**, *120*, 5940−5948.

(8) Knauf, R. R.; Brennaman, M. K.; Alibabaei, L.; Norris, M. R.; Dempsey, J. L. Revealing the Relationship Between Semiconductor Electronic Structure and Electron Transfer Dynamics at Metal Oxide−Chromophore Interfaces. *J. Phys. Chem. C* **2013**, *117*, 25259−25268.

(9) Green, A. N. M.; Palomares, E.; Haque, S. A.; Kroon, J. M.; Durrant, J. R. Charge Transport Versus Recombination in Dye-Sensitized Solar Cells Employing Nanocrystalline TiO_2 and SnO_2 Films. *J. Phys. Chem. B* **2005**, *109*, 12525−12533.

(10) Wee, K.-R.; Sherman, B. D.; Brennaman, M. K.; Sheridan, M. V.; Nayak, A.; Alibabaei, L.; Meyer, T. J. An Aqueous, Organic Dye Derivatized SnO_2/TiO_2 Core/Shell Photoanode. *J. Mater. Chem. A* **2016**, *4*, 2969−2975.

(11) Sherman, B. D.; Ashford, D. L.; Lapides, A. M.; Sheridan, M. V.; Wee, K.-R.; Meyer, T. J. Light-Driven Water Splitting with a Molecular Electroassembly-Based Core/Shell Photoanode. *J. Phys. Chem. Lett.* **2015**, *6* (16), 3213−3217.

(12) Kavan, L.; Grätzel, M.; Gilbert, S. E.; Klemenz, C.; Scheel, H. J. Electrochemical and Photoelectrochemical Investigation of Single-Crystal Anatase. *J. Am. Chem. Soc.* **1996**, *118*, 6716−6723.

(13) Scanlon, D. O.; Dunnill, C. W.; Buckeridge, J.; Shevlin, S. A.; Logsdail, A. J.; Woodley, S. M.; Catlow, C. R. A.; Powell, M. J.; Palgrave, R. G.; Parkin, I. P.; et al. Band Alignment of Rutile and Anatase TiO_2. *Nat. Mater.* **2013**, *12*, 798−801.

(14) Milot, R. L.; Moore, G. F.; Crabtree, R. H.; Brudvig, G. W.; Schmuttenmaer, C. A. Electron Injection Dynamics from Photoexcited Porphyrin Dyes into SnO_2 and TiO_2 Nanoparticles. *J. Phys. Chem. C* **2013**, *117*, 21662−21670.

(15) Kafizas, A.; Wang, X.; Pendlebury, S. R.; Barnes, P.; Ling, M.; Sotelo-Vazquez, C.; Quesada-Cabrera, R.; Li, C.; Parkin, I. P.; Durrant, J. R. Where Do Photogenerated Holes Go in Anatase:Rutile TiO_2? A Transient Absorption Spectroscopy Study of Charge Transfer and Lifetime. *J. Phys. Chem. A* **2016**, *120*, 715−723.

(16) Park, N. G.; van de Lagemaat, J.; Frank, A. J. Comparison of Dye-Sensitized Rutile- and Anatase-Based TiO_2 Solar Cells. *J. Phys. Chem. B* **2000**, *104*, 8989−8994.

(17) Lapides, A. M.; Sherman, B. D.; Brennaman, M. K.; Dares, C. J.; Skinner, K. R.; Templeton, J. L.; Meyer, T. J. Synthesis, Characterization, and Water Oxidation by a Molecular Chromophore-Catalyst Assembly Prepared by Atomic Layer Deposition. The "Mummy" Strategy. *Chem. Sci.* **2015**, *6*, 6398−6406.

(18) Swierk, J. R.; McCool, N. S.; Saunders, T. P.; Barber, G. D.; Strayer, M. E.; Vargas-Barbosa, N. M.; Mallouk, T. E. Photovoltage Effects of Sintered IrO_2 Nanoparticle Catalysts in Water-Splitting Dye-Sensitized Photoelectrochemical Cells. *J. Phys. Chem. C* **2014**, *118*, 17046−17053.

(19) Hanson, K.; Brennaman, M. K.; Luo, H.; Glasson, C. R. K.; Concepcion, J. J.; Song, W.; Meyer, T. J. Photostability of Phosphonate-Derivatized, Ru(II) Polypyridyl Complexes on Metal Oxide Surfaces. *ACS Appl. Mater. Interfaces* **2012**, *4*, 1462−1469.

(20) Hanson, K.; Losego, M. D.; Kalanyan, B.; Ashford, D. L.; Parsons, G. N.; Meyer, T. J. *Chem. Mater.* **2013**, *25*, 3−5.

(21) McCool, N. S.; Swierk, J. R.; Nemes, C. T.; Saunders, T. P.; Schmuttenmaer, C. A.; Mallouk, T. E. Proton-Induced Trap States, Injection and Recombination Dynamics in Water-Splitting Dye-Sensitized Photoelectrochemical Cells. *ACS Appl. Mater. Interfaces* **2016**, *8*, 16727−16735.

(22) Abrahamsson, M.; Johansson, P. G.; Ardo, S.; Kopecky, A.; Galoppini, E.; Meyer, G. J. Decreased Interfacial Charge Recombination Rate Constants with N3-Type Sensitizers. *J. Phys. Chem. Lett.* **2010**, *1*, 1725−1729.

(23) Swierk, J. R.; Méndez-Hernández, D. D.; McCool, N. S.; Liddell, P.; Terazono, Y.; Pahk, I.; Tomlin, J. J.; Oster, N. V.; Moore, T. A.; Moore, A. L.; et al. Metal-Free Organic Sensitizers for Use in Water-Splitting Dye-Sensitized Photoelectrochemical Cells. *Proc. Natl. Acad. Sci. U. S. A.* **2015**, *112*, 1681−1686.

DOI: 10.1021/acsenergylett.6b00279
ACS Energy Lett. 2016, 1, 603−606

Supporting Information for:

Rutile TiO_2 as an Anode Material for Water-Splitting Dye-Sensitized Photoelectrochemical Cells

John R. Swierk*, Kevin P. Regan, Jianbing Jiang, Gary W. Brudvig, Charles A. Schmuttenmaer*

Department of Chemistry and Yale Energy Sciences Institute, Yale University, New Haven, CT 06520-8107, United States

Experimental Procedures

(4,4'-diphosphonato-2,2'-bipyridine)bis(2,2'-bipyridine)ruthenium(II) bromide (**RuP**) was prepared according to literature procedures.[1]

1. Preparation of Rutile TiO_2 films

The films were prepared following a modification of the technique developed by Park et al.[2] and McCool et al.[3] $TiCl_4$ (5.48 mL, 0.05 mol) was added to 25 mL of water in a glass bottle to give a 2 M solution, which was immediately diluted to 100 mL. The bottle was capped and allowed to stir at room temperature for 5 days, giving a milky white suspension. The solution was sonicated in an ice bath using an ultrasonic horn for 15 minutes and then allowed to settle for 3 hours to remove any large aggregates. Following settling, the suspension was centrifuged at 5500 rpm for 15 minutes to aggregate the particles. After centrifugation, the particles were washed with ethanol three times by using ultrasonication to resuspend the particles in the ethanol followed by centrifugation at 5500 rpm for 30 min. Following the third wash, a solution of 1.45 g of ethyl cellulose and 13.6 g of α-terpineol in 73 mL of ethanol was added, followed by 15 minutes of ultrasonicating to suspend the particles. The ethanol was stripped by rotary evaporation to give a paste.

Films of r-TiO_2 were prepared on FTO glass (TEC15, Hartford glass) using Scotch Magic tape as a spacer for doctor-blading. One layer of tape was found to give a nominal layer thickness (after sintering) of 3.5 μm. Solaronix Ti-Nanoxide T/SP was used for a-TiO_2 films, with one layer of tape giving a nominal thickness of 3.5 μm. After the initial layer, the films were allowed to cure at 80 °C for 10 minutes before the second layer was applied. Films were sintered in a box furnace in air using the following heating profile: 180 °C/hour to 370 °C, hold at 370 °C for 5 minutes, 180 °C/hour to 470 °C, 10 minutes at 470 °C, followed by cooling to room temperature at 600 °C/hour. For dye-sensitized films, the sintered r-TiO_2 and a-TiO_2 films were immersed in a 0.1 mM solution of RuP in ethanol for 22 hours. Sensitized a-TiO_2 films were coated with ~4Å of Al_2O_3 as previously described.[4]

A FEI Osiris was used for TEM analysis of the sintered r-TiO_2 powder.

X-ray diffraction data were collected at room temperature using a P-XRD Brunker D8 Focus Powder X-ray Diffractometer. The XRD spectrum and its associated JCPDS (No. 76-1940) are presented in Figure S1. The Scherrer equation was used to estimate the particle size of the r-TiO_2:

$$\tau = \frac{K\lambda}{\beta \cos\theta} \tag{1}$$

where K is the shape factor (we assume is 0.9)[5], λ is the wavelength of the X-ray source (1.5056 Å), β is the full width at half maximum (FWHM) of an isolated XRD peak (in radians), and θ corresponds to the Bragg angle. It was found that the peak shape was best described by a Lorentzian function with an offset:

$$L(2\theta) = \frac{A}{(2\theta - 2\theta_o)^2 + \left(\frac{\Gamma}{2}\right)^2} + L_o \tag{2}$$

where A is the amplitude, $2\theta_0$ is the angle of the reflected beam, Γ is the FWHM of the XRD peak, and L_0 accounts for any baseline offset in the spectrum. The best fit parameters of the Lorentzian-like peak are presented in Figure S2.

2. Transient-Absorption Spectroscopy

Transient-absorption data were collected using an Edinburgh Instruments LP900 spectrometer. The samples were pumped at 532 nm an Nd:YAG laser (SpectraPhysics, INDI-10) utilizing the third harmonic (355 nm) passed through an optical parametric oscillator (OPO, SpectraPhysics) to generate a 3 mJ, 10 mm diameter, 532 nm pulse. The samples were immersed in a solution of 0.1 M KNO_3 for transient-absorption measurements. A pulsed 450 W Xe arc lamp was filtered with a 420 nm longpass filter and utilized as the probe source. Following the sample, the probe source was passed through a monochromator to selectively monitor 440 nm light on a photomultiplier tube.

Injection yields were estimated by monitoring the bleach at t = 0. Briefly, the difference in the extinction coefficient at 440 nm for Ru(III) (4528 M^{-1} cm^{-1}) was estimated by holding RuP-sensitized r-TiO_2 at 1.5 V vs Ag/AgCl in 0.1 M $HClO_4$ to fully oxidize the film. The absorption at 532 nm was found by subtracting the absorption spectrum of the r-TiO_2 film prior to sensitization. Only sensitizers that inject an electron and are oxidized contribute to the change in absorbance; thus, the bleach at t = 0 corresponds only to sensitizers that inject into r-TiO_2. The injection yield is found by dividing the number of oxidized RuP sites by the total number of photons absorbed at 532 nm.

3. Photoelectrochemical Experiments

Bulk photoelectrolysis experiments were carried out in an H-cell configuration with one compartment holding the photoanode and a Ag/AgCl reference electrode and the other compartment holding a Pt mesh counter electrode. The buffer used for photoelectrochemical

experiments was a pH 6.8 potassium phosphate buffer with 0.5 M KNO_3 as a supporting electrolyte and 20 mM hydroquinone added as a reductive scavenger. Illumination was provided by a 300 W Xe arc lamp fitted with an AM1.5 filter, and also a 420 nm longpass filter for some experiments.

Sample Calculation for Injection Yield

$$PulseIntensity = 1.02x10^{16}\ \frac{photons}{cm^2}$$

$$Abs_{532nm} = 0.051$$

$$Absorbed\quad Photons = 8.70x10^{14}\ \frac{photons}{cm^2}$$

$$\Delta\varepsilon_{Ru(III)} = 6300\quad M^{-1}cm^{-1}$$

$$\Delta A_{t=0} = 0.0085$$

$$Ru(III)\quad formed = 0.0085 \times \frac{1}{6300 M^{-1}cm^{-1}} \times \frac{1L}{1000 cm^{-3}} \times \frac{6.023x10^{23}}{mol} = 8.13x10^{14}\ cm^{-2}$$

$$Injection\,Yield = \frac{8.13x10^{14}\ cm^{-2}}{8.70x10^{14}\ cm^{-2}} = 0.91$$

The estimated injection yield is first calculated by finding the total number of photons in the laser pulse, followed by the total number of absorbed photons (determined from the difference between the scattering baseline of the unsensitized film and the sensitized film). The number of injected electrons is determined from the change in absorbance at time zero, corresponding to the formation of Ru(III) upon injection. Assuming an extinction coefficient of 6300 M^{-1} cm^{-1} (determined from spectroelectrochemical measurements) the total number of injected electrons is determined. Finally, the injection yield is found by dividing the number of injected electron determined from the bleach at t=0 by the number of absorbed photons.

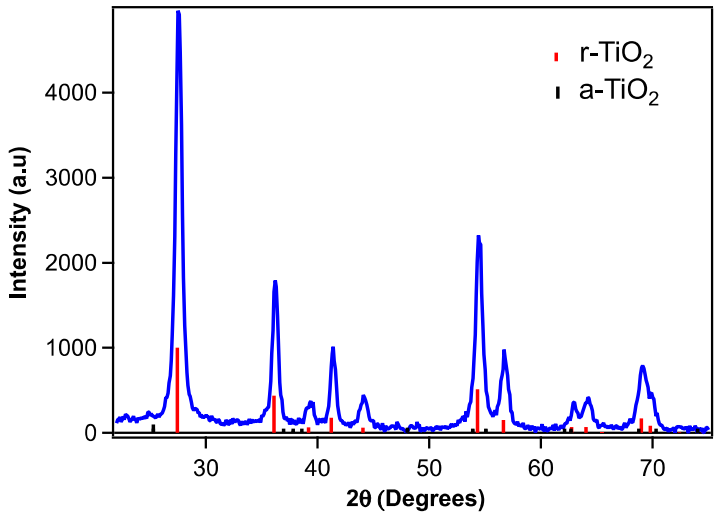

Figure S1: Powder X-ray diffraction of a sintered rutile TiO_2 film.

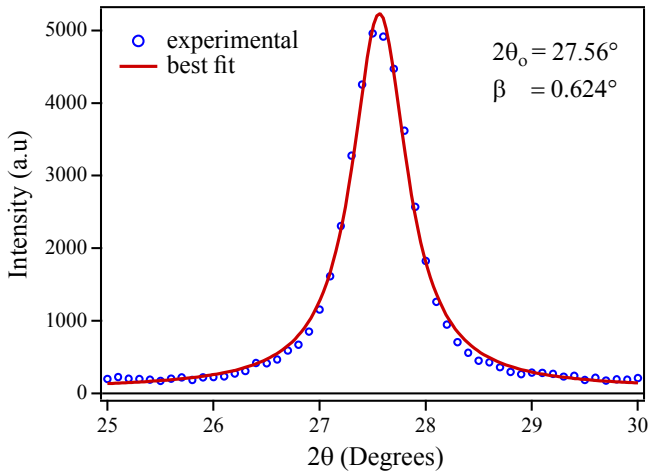

Figure S2: Isolated XRD peak fit to equation 2.

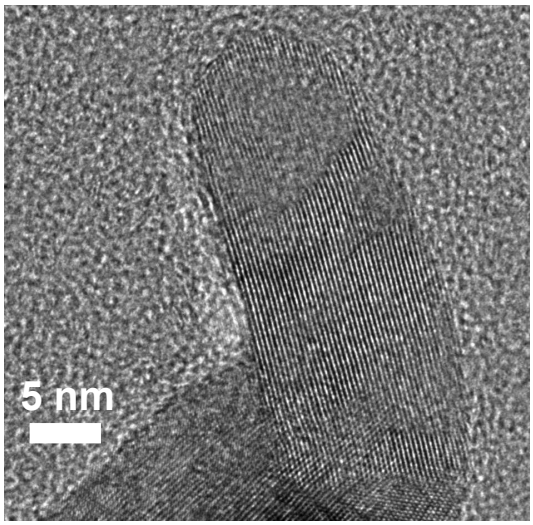

Figure S3: Transmission electron micrograph of rutile TiO_2 particle.

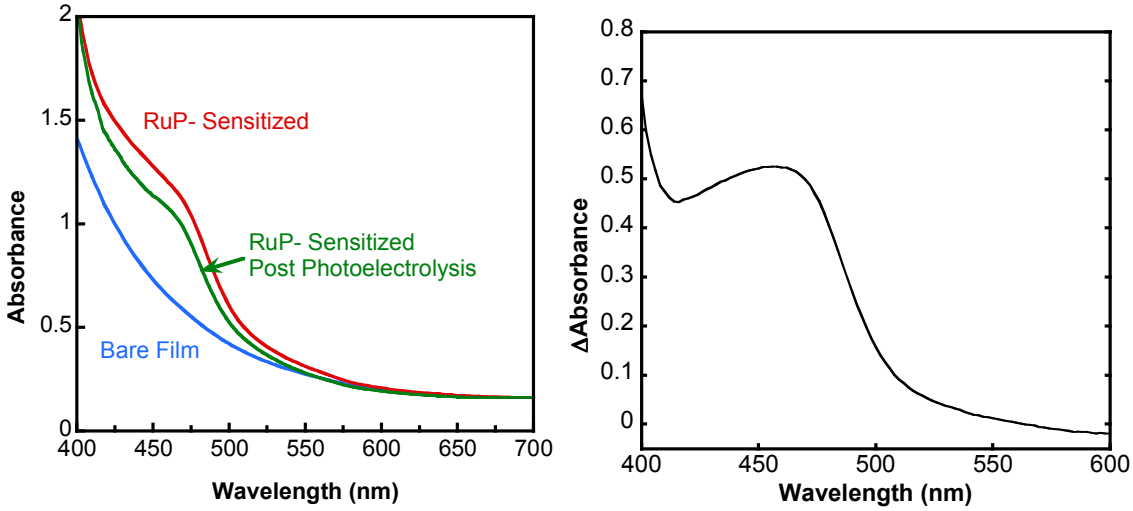

Figure S4: (Left) UV-visible spectra of bare (blue) and RuP-sensitized (red) rutile TiO_2 film. (Right) Absorption difference between bare and RuP-sensitized film showing contribution to absorption of just RuP.

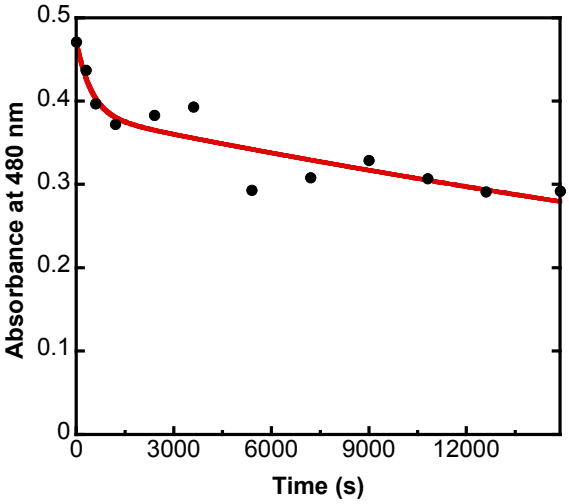

Figure S5: Change in absorption of RuP-sensitized r-TiO_2 with time in 0.1 M KNO_3 illuminated in air by a 470 nm LED (irradiation of 475 mW cm^{-2}). Absorption is relative to the bare r-TiO_2 film to correct for scattering.

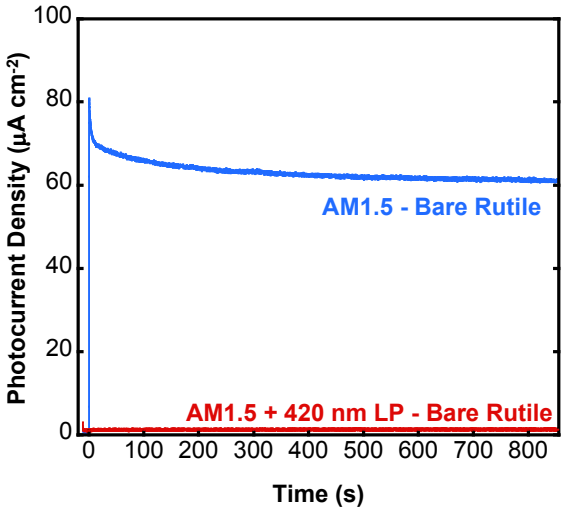

Figure S6: Chronoamperometry of a bare rutile TiO_2 film illuminated with a 300 W Xe lamp fitted with an AM1.5 filter (blue trace) and an AM1.5 filter plus a 420 nm longpass filter (red trace) as well as a RuP-sensitized anatase TiO_2 film. Samples are in a pH 6.8 potassium phosphate buffer with 0.5 M KNO_3 and 20 mM hydroquinone added.

References

1. Gillaizeau-Gauthier, I.; Odobel, F.; Alebbi, M.; Argazzi, R.; Costa, E.; Bignozzi, C. A.; Qu, P.; Meyer, G. J. *Inorg. Chem.* **2001**, *40*, 6073–6079.

2. Park, N-G., J. Van de Lagemaat, and A. J. Frank. *J. Phys. Chem. B* **2000**, *104*, 8989–8994.

3. McCool, N. S.; Swierk, J. R.; Nemes, C. T.; Saunders, T. P.; Schmuttenmaer, C. A.; Mallouk, T. E. *ACS Appl Mater Interfaces* **2016**, *8*, 16727-16735.

4. Swierk, J. R.; McCool, N. S.; Nemes, C. T.; Mallouk, T. E.; Schmuttenmaer, C. A. *J. Phys. Chem. C* **2016**, *120*, 5940–5948.

5. Hou, Y.; Li, X-Y; Zhao, Q-D; Quan, X, Chen, G-H, *Adv. Func. Mater.*, **2010**, *20*, 2165-2174.